



Microsensor and transcriptomic signatures of oxygen depletion in biofilms associated with chronic wounds

Authors: Garth A. James, Alice Ge Zhao, Marcia Usui, Robert A. Underwood, Hung Nguyen, Haluk Beyenal, Elinor deLancey Pulcini, Alessandra Agostinho Hunt, Hans C. Bernstein, Philip Fleckman, John Olerud, Kerry S. Williamson, Michael J. Franklin, & Philip S. Stewart

This is the peer reviewed version of the following article: citation below, which has been published in [Wound Repair and Regeneration](#) and in final form at <https://dx.doi.org/10.1111/wrr.12401>. This article may be used for non-commercial purposes in accordance with Wiley Terms and Conditions for Self-Archiving.

James, Garth A. , Alice Ge Zhao, Marcia Usui , Robert A. Underwood, Hung Nguyen, Haluk Beyenal, Elinor deLancey Pulcini, Alessandra Agostinho Hunt, Hans C. Bernstein, Philip Fleckman, John Olerud, Kerry S. Williamson, Michael J. Franklin, and Philip S. Stewart. "Microsensor and transcriptomic signatures of oxygen depletion in biofilms associated with chronic wounds." *Wound Repair and Regeneration* 24, no. 2 (March/April 2016): 373-383. DOI: 10.1111/wrr.12401.

Made available through Montana State University's [ScholarWorks](http://scholarworks.montana.edu)
scholarworks.montana.edu

Microsensor and transcriptomic signatures of oxygen depletion in biofilms associated with chronic wounds

Garth A. James, PhD¹; Alice Ge Zhao, MD²; Marcia Usui, BS²; Robert A. Underwood, BFA²; Hung Nguyen, PhD³; Haluk Beyenal, PhD³; Elinor deLancey Pulcini, PhD¹; Alessandra Agostinho Hunt, PhD⁴; Hans C. Bernstein, PhD⁵; Philip Fleckman, MD²; John Olerud, MD²; Kerry S. Williamson, BS¹; Michael J. Franklin, PhD¹; Philip S. Stewart, PhD¹

1. Center for Biofilm Engineering, Montana State University, Bozeman, Montana,
2. Division of Dermatology, Department of Medicine, University of Washington, Seattle, Washington,
3. The Gene and Linda Voiland School of Chemical Engineering and Bioengineering, Washington State University, Pullman, Washington,
4. Department of Microbiology and Molecular Genetics, 5180 Biomedical and Physical Sciences, Michigan State University, East Lansing, Michigan,
5. Pacific Northwest National Laboratory, Chemical and Biological Signature Science, Richland, Washington

Abstract

Biofilms have been implicated in delayed wound healing, although the mechanisms by which biofilms impair wound healing are poorly understood. Many species of bacteria produce exotoxins and exoenzymes that may inhibit healing. In addition, oxygen consumption by biofilms and by the responding leukocytes, may impede wound healing by depleting the oxygen that is required for healing. In this study, oxygen microsensors to measure oxygen transects through in vitro cultured biofilms, biofilms formed in vivo within scabs from a diabetic (db/db) mouse wound model, and ex vivo human chronic wound specimens was used. The results showed that oxygen levels within mouse scabs had steep gradients that reached minima ranging from 17 to 72 mmHg on live mice and from 6.4 to 1.1 mmHg on euthanized mice. The oxygen gradients in the mouse scabs were similar to those observed for clinical isolates cultured in vitro and for human ex vivo specimens. To characterize the metabolic activities of the bacteria in the mouse scabs, transcriptomics analyses of *Pseudomonas aeruginosa* biofilms associated with the db/db mice wounds was performed. The results demonstrated that the bacteria expressed genes for metabolic activities associated with cell growth. Interestingly, the transcriptome results also indicated that the bacteria within the wounds experienced oxygen-limitation stress. Among the bacterial genes that were expressed in vivo were genes associated with the Anr-mediated hypoxia-stress response. Other bacterial stress response genes highly expressed in vivo were genes associated with stationary-phase growth, osmotic stress, and RpoH-mediated heat shock stress. Overall, the results supported the hypothesis that bacterial biofilms in chronic wounds promote chronicity by contributing to the maintenance of localized low oxygen tensions, through their metabolic activities and through their recruitment of cells that consume oxygen for host defensive processes.

Local oxygen concentration has long been recognized as a critical parameter in wound healing.^{1,2} Tissue oxygenation in the vicinity of a wound correlates positively with wound healing² and very low oxygen levels are often measured around nonhealing wounds. Skin oxygenation is commonly measured as transcutaneous oxygen tension (TcPO₂). Whereas TcPO₂ is typically 70 mmHg in healthy skin, in the extremities of patients with impaired healing ulcers, TcPO₂ can be a small fraction of this concentration. For example Kalani et al.,³ measured TcPO₂ in 50 diabetic patients with chronic foot ulcers. In the group exhibiting impaired wound healing, TcPO₂ at the dorsum of the foot averaged 13 mmHg whereas it was 60 mmHg at a reference point on the chest. In a study of ulcer healing in patients

with critical limb ischemia Ruangsetakit et al.,⁴ reported that none of the patients with TcPO₂ less than 20 mmHg showed signs of ulcer healing, whereas all of the patients with a TcPO₂ greater than 40 mmHg showed a progression toward healing during the study period. The poor healing of ischemic wounds underscores the importance of oxygen supplied to the wound via blood circulation. This is the primary source of the wound oxygen supply.²

Poor tissue oxygenation near a wound increases the risk of wound infection.⁵ For example, in a study of 130 operative general surgery patients at notable risk of infection, tissue oxygenation was a strong predictor of postoperative wound infection.⁶ An indirect indication of the very low oxygen concentration in chronic wounds is the recovery of

strict anaerobic bacteria from these ulcers. Anaerobes have occasionally been cultured⁷ and more recently have been identified by sequencing of bacterial DNA in specimens from chronic wounds.⁸

Pseudomonas aeruginosa is an opportunistic pathogen that causes acute and chronic biofilm-associated infections. *P. aeruginosa* biofilms have been associated with non-healing wounds.⁹ Previous animal studies have shown that chronic wounds infected with *P. aeruginosa* showed impaired wound closure rates in diabetic mice¹⁰ and in a rabbit ear model¹¹ and a greater degree of polymorphonuclear inflammation in BALB/c mice.¹² To determine the effects of *P. aeruginosa* biofilms on healing of diabetic ulcers, a wound infection model with diabetic (db/db) mice and *P. aeruginosa* biofilms was developed.^{13,14} Biofilms were applied 2 days post wounding and then both inoculated and control wounds were covered with a semi-occlusive dressing, which was left in place for 17 days. Exudate material, such as fluid, cells, or cellular debris accumulated under the dressings. When the dressings were removed, the exudates dried to form scabs (crusts of dried blood, serum, and exudate) over the wounds. Viable *P. aeruginosa* persisted in the infected wounds and could be isolated from the wounds 28 days postinoculation ($\sim 10^7$ cells/wound), with most of the bacteria associated with the scab rather than the wound bed. The presence of infiltrating neutrophils was noted in both the scab and wound bed of the wounds infected with *P. aeruginosa* biofilms. The results indicated that the presence of *P. aeruginosa* biofilms delayed wound healing by at least 2 weeks and that the biofilms caused increased levels of inflammatory cytokines and reduced vascularization. Delayed wound healing and persistence of infection may be due to the ability of *P. aeruginosa* to encode a number of virulence factors, such as toxins, proteases, and lipases, that allow the bacteria to obtain nutrients and survive host defenses. Furthermore, the persistence of *P. aeruginosa*, or other bacteria, as biofilms in wounds may compromise host defenses, particularly neutrophil response. The respiratory burst of the neutrophils likely reduces oxygen concentrations within the wounds.¹⁵ However, direct oxygen consumption by biofilms may also be an important contributor to reduced oxygen concentrations and poor healing of chronic wounds.

In this study, we sought to test the hypothesis that bacterial biofilms contribute to the establishment and maintenance of low localized oxygen tensions in wounds. This effect may be direct and due to oxygen consumption by bacterial respiration or indirect and due to the response of oxygen-consuming host cells that respond to the presence of the biofilm. The latter case may be particularly relevant for *P. aeruginosa* infected wounds where neutrophil accumulation and associated tissue damage may be more detrimental than the direct effects of the bacteria.¹⁶ Nonetheless, other species of bacteria, such as *Staphylococcus aureus* that did not elicit an equivalent neutrophil response to *P. aeruginosa*¹⁶ often colonize or infect chronic wounds. Furthermore, wound biofilms are often polymicrobial with numerous species consuming oxygen and promoting anoxia. If this hypothesis is supported, it could help explain the persistent hypoxic state of many chronic wounds, and the association between the presence of a biofilm and poor wound healing. Here, we used oxygen microsensors to measure oxygen concentrations of in vitro cultured biofilms composed of clinical isolates, biofilms in mouse wounds infected with *P. aeruginosa*,

and wound specimens excised from human subjects. We also characterized the persistence of *P. aeruginosa* activity within biofilms in the mouse wound model by isolating and identifying mRNA from the wounds 28 days postinfection and performing transcriptome analysis of the biofilm bacteria. The microsensor and transcriptomics results indicated that chronic wounds with *P. aeruginosa* biofilms had a persistent hypoxic state. These results suggest that poor healing of chronic wounds may be due, in part, to the activity of biofilms which cause reduction of the oxygen partial pressure of the wound.

MATERIALS AND METHODS

Bacterial strains and culture conditions

Human clinical isolates were obtained from the South West Regional Wound Care Center, Lubbock Texas where they were isolated from wounds of subjects undergoing sharp debridement as part of standard wound care management, with approval from the Western Institutional Review Board for the Protection of Human Subjects. For this study, the clinical isolates *Staphylococcus aureus* 10943, *P. aeruginosa* 215, and *Enterococcus faecalis* 384 were used as inocula for in vitro biofilm formation. Isolates were stored at -70°C as 1 mL frozen stock cultures in peptone glycerol. Overnight cultures were grown by placing a frozen stock culture in 10 mL tryptic soy broth (TSB) and incubating at 37°C for approximately 16 hours. The overnight cultures were then diluted with fresh TSB to an optical density of 0.05 at 600 nm to produce inocula. For multispecies experiments, equal volumes of diluted *P. aeruginosa*, *S. aureus*, and *E. faecalis* inocula were combined.

Although, human clinical isolates were used for the in vitro experiments, a well-characterized strain, *P. aeruginosa* mPAO1, with previously published planktonic and biofilm transcriptome data was used for the in vivo mouse infection model. *P. aeruginosa* mPAO1 was obtained from the University of Washington Genome Center (www.genome.washington.edu/UWGC). This strain of *P. aeruginosa* has a published genome sequence, a mutant library available from the Genome Center, and was used to develop the mouse biofilm infected wound model in previous research.^{13,14} Frozen stock cultures of PAO1 were grown overnight in LB medium at 37°C on a shaker. The PAO1 culture was diluted 1:1,000 in sterile phosphate buffer solution (PBS) to produce inocula.

Collection and analysis of human chronic wound specimens

Human wound specimens were collected from subjects undergoing sharp debridement as part of standard wound management at Bozeman Health Wound and Lymphedema Center with approval from the Montana State University Institutional Review Board. Debridement was performed using a 3-mm curette. Samples were placed on blood agar plates and transported to the laboratory. The samples were then cut into two pieces; one piece was frozen for DNA extraction while the other was left on the blood agar plate and equilibrated for 12 hours at 37°C prior to oxygen microsensor profiling, as described below. For sequence analysis, samples were placed in bead beater tubes and processed at maximum speed 6.5 for 45 seconds using the

FastPrep FP120 Bead Beater (Savant Instruments Inc., Farmingdale, NY). DNA was then extracted from the samples following protocols for the FAST Spin Prep Kit for Soil (MP BioMedicals, Santa Ana, CA). Amplification of bacterial DNA was performed using the 16S rDNA Primers 8F (AGAGTTTGATCCTGGCTCAG) and 1492R (GGTTACCTTGTTACGACTT) (Integrated DNA Technologies, Coralville, IA). Confirmation of amplified DNA products of the correct size was confirmed using agarose gels stained with GelRed Nucleic Acid Stain (Biotium Inc., Hayward, CA). PCR products were purified using a PCR Product Clean Up kit (Qiagen Inc., Valencia, CA) and cloned with a TOPO TA Cloning Kit (Invitrogen, Carlsbad, CA). Transformed cells were spread plated on Tryptic Soy Agar amended with 50 µg/mL ampicillin and incubated overnight at 37°C. White colonies were picked from plates and cultured in separate tubes of LB medium, amended with 50 µg/mL kanamycin, for 24 hours at 37°C. Plasmid preparation was performed on turbid samples using the PureLink Quick Plasmid Miniprep Kit (Invitrogen) following the manufacturer's protocols. Purified plasmids were sent to Laragen Inc. (Culver City, CA) for Sanger sequencing. Returned sequences were analyzed using BLASTn (Pub Med).

Colony biofilm model (CBM)

The CBM is an in vitro method that has been used to investigate antimicrobial tolerance of biofilms.¹⁷ Colony biofilms were grown on black, polycarbonate, 0.22 µm pore-size, 25 mm diameter, disk filter membranes (Osmonics, Inc, Minnetonka, MN). Prior to inoculation, the membranes were sterilized in a laminar flow hood under germicidal light for 10–15 minutes on each side. Sterile membranes were placed on Blood Agar plates using forceps, with the shiny side of the membrane facing up. The membranes were inoculated by pipetting 10 µL aliquots of inoculum onto each membrane. The inoculated membranes were allowed to dry for 15–30 minutes. Then, the plates were placed in a 37 °C incubator for 72 hours, with aseptic transfers to fresh Blood Agar plates at 24 and 48 hours.

Enumeration of colony forming units (CFUs)

Viable cells were enumerated by serial diluting and plating replicate samples of biofilms for which oxygen profiles were collected. The membranes were placed in 10 mL of sterile PBS and then vortexed (30 seconds), sonicated (2 minutes), and vortexed again (30 seconds). Serial 10-fold dilutions were then made using sterile PBS. Single species biofilms were plated on Tryptic Soy Agar (TSA, Difco Becton Dickinson and Company, Sparks, MD). Mixed-species biofilms were plated on selective agar. For *E. faecalis* counts, samples were plated on Mitis–Salivarius Agar (Difco Becton Dickinson and Company, Sparks, MD) and incubated anaerobically for two days at 37°C. For *P. aeruginosa* counts, the samples were plated on Pseudomonas Isolation Agar (Difco Becton Dickinson and Company, Sparks, MD), and for *S. aureus* counts, the samples were plated on Staphylococcus Medium 110 (Difco Becton Dickinson and Company, Sparks, MD). For *P. aeruginosa* and *S. aureus* counts, the plates were incubated at 37°C under aerobic conditions. After incubation, the plates were counted and the number of colony forming

units (CFU) for each sample was calculated and log(10)-transformed.

Biofilm thickness measurements

Membranes with biofilms were embedded in Optimum Cutting Temperature (OCT, Sakura Finetek, Torrance, CA), frozen on dry ice, and stored at –70°C in preparation for cryosectioning. The samples were then sliced into 5 µm cross-sections using the Leica CM 1850 Cryostat (Leica, Wetzlar, Germany), placed on Superfrost Plus slides (Fisher Scientific, Pittsburg, PA). The sections were examined with transmitted light using a Nikon Eclipse E800 microscope and images were collected with an Olympus Q-color 5 camera (Olympus, Center Valley, PA). Thickness measurements were performed using MetaMorph software (Molecular Devices, LLC, Sunnyvale, CA).

Biofilm infection in the murine wound model

The mouse model was developed to study chronic wounds infected with *P. aeruginosa* biofilms in diabetic (db/db) mice and has been described in detail.^{13,14} The studies were conducted with the University of Washington Institutional Animal Care and Use Committee approval in compliance with the NIH guide for the Care and Use of Laboratory Animals, 1996. Briefly, 6-mm punch biopsy wounds were created on the dorsal surface of diabetic (db/db) mice, subsequently infected with *P. aeruginosa* (PAO1) biofilms 2 days postwounding, and covered with semi-occlusive dressings (Tegaderm, 3M, St. Paul, MN) for 2 weeks. The biofilm cultivation method for these experiments was based on the CBM described above. The polycarbonate membrane filters were cut using a 6-mm biopsy punch (Acuderm, Inc., Ft. Lauderdale, FL), and sterilized with exposure to UVC light for 5 minutes on both sides. The filters were inoculated with 2 µL of PAO1 and incubated at 37 °C for 72 hours, with transfer to fresh LB agar plates at 24 and 48 hours prior to application to the wound.

Oxygen concentration measurements for wound and biofilm transects

All oxygen measurements were performed using amperometric microsensors. For measurements within in vitro biofilms and the mouse wounds, custom microsensors were constructed and calibrated as described by Lewandowski and Beyenal.¹⁸ Movement of the microsensors was controlled by a Mercury-step motor controller (PI M-230.10S Part No. M23010SX, Physik Instrumente, Auburn, MA) and by custom Microprofiler software. In each measurement, the microsensor was moved downward from the air to the biofilm or wound by a step of 10 µm. Data were recorded on a Dell laptop using an Analog/Digital Converter (ADC, Measurement Computing USB-1608FS, Norton, MA). For measurements of oxygen concentrations within human wound debridement specimens, commercially available microsensors were used (OX microsensors Unisense A/S, DK). A Unisense multimeter coupled with SensorTrace (Unisense A/S, Denmark) software was used for signal amplification and data collection. The microsensors were positioned with a standard micromanipulator with manual XYZ positioning, a motorized stage, a mounting stage, and motor controller. The microsensors were depolarized for at least 5 hours before use and a two point

calibration was performed immediately before use. Calibration standards consisted of an anoxic standard (deionized water containing 100 mM NaOH and 100 mM ascorbic acid) and an oxic standard (air-saturated deionized water).

RNA extraction and quality control

Scabs from wounds infected with PAO1 from two mice were surgically excised at 28 days and the duplicate specimens were processed independently. Each scab was collected and stored in 1 mL of RNeasy Lysis Buffer (Qiagen) at -20°C . Two separate 72 hour colony biofilms, prepared as those used for wound inoculation, were collected in the same manner. RNA was extracted using an Aurum Total RNA Fatty and Fibrous Tissue Kit (Bio-Rad, Hercules, CA). RNA quality was verified on a Bioanalyzer 2100 Nanochip (Agilent, Santa Clara, CA). Total RNA was quantified on the Nanodrop 1000 (Nanodrop Technologies, Wilmington, DE). *P. aeruginosa* specific rRNA from the total RNA was analyzed by RT-qPCR of the 16S rRNA. Primer sequences and concentrations for *P. aeruginosa* 16S rRNA were described previously.¹⁹ RT-qPCR was performed using the one-step QuantiTect Probe RT-PCR kit (Qiagen) and the Rotorgene 6000 instrument (Corbett Research, San Francisco, CA). RNA extracted from a colony biofilm was used to construct a standard curve over five orders of magnitude. Controls lacking reverse transcriptase indicated that the RNA was free from interfering levels of DNA.

cDNA synthesis and preparation

One microliter of Poly-A control RNA (Affymetrix, Santa Clara, CA), diluted to the manufacturer's specifications, was added to purified RNA from each scab sample and from two biofilm wound inoculum samples. The RNA was reverse transcribed at 42°C overnight using 1 μL random primers (Invitrogen), 1 μL Superase-In (Ambion, Carlsbad, CA), 6 μL 5 \times first strand buffer (Invitrogen), 3 μL 0.1 M DTT, 0.6 μL 100 mM dNTPs (Invitrogen), and 3 μL Superscript II (Invitrogen). After synthesis, the remaining RNA was hydrolyzed by the addition of 0.5 M EDTA and 1 N sodium hydroxide. The cDNA samples were neutralized with 1 N HCl and 1 M sodium acetate. The reactions were then cleaned on MinElute columns (Qiagen) according to the manufacturer's instructions. The resulting cDNA was fragmented with 0.6 Units DNase I (GE Healthcare, Wauwatosa, WI) per microgram cDNA for 10 minutes at 37°C . The enzyme was inactivated by heating to 98°C for 10 minutes. The resulting cDNA fragment sizes, assessed using an Agilent RNA 6000 nano assay (Agilent, Santa Clara, CA), ranged from 25 to 120 nucleotides in length. Fragmented cDNA was terminally labeled by incubation with 10 μL 5 \times reaction buffer, 2 μL GeneChip DNA labeling reagent (Affymetrix, Santa Clara, CA), and 2 μL terminal deoxynucleotidyl transferase (Promega, Madison, WI) for 60 minutes at 37°C .

Hybridization, scanning, and statistical analysis of microarray data

Labeled cDNA was hybridized for 16 hours at 50°C with constant rotation to Affymetrix *P. aeruginosa* microarrays (part #900640). Microarrays were washed and stained using a GCOS Fluidics Station 450 and scanned with an Affymetrix 7G scanner. Affymetrix GCOS v1.4 was used to gener-

ate CEL and CHP files. CEL files were imported into FlexArray v1.6.1 for QC and data analysis.²⁰ For scab transcriptome analysis, the RMA algorithm was applied to the arrays, which included background correction, quantile normalization, and median polishing. A signal intensity (SI) filter was applied to the normalized data to select transcripts with $\text{SI} > 2^6$ in both arrays. For transcripts meeting this SI requirement in both arrays, the average SI was calculated and the top 5% (285) of transcripts were selected for further analysis. This gene list was uploaded in to "The Database for Annotation, Visualization and Integrated Discovery (DAVID)" for identification of enriched biological themes with the functional annotation clustering tool.²¹ The gene list was also compared with lists of genes associated with particular responses or activities, compiled from the literature as documented in Supporting Information Table S2. For overlap analysis, *p*-values for assessing the statistical significance of gene set enrichment were calculated using a negative binomial distribution.²² For comparative analysis of the wound inoculums and scab, Principal Component Analysis (PCA) was used to enable visualization, assessment, and grouping of the data. Data were compared with previously published *Pseudomonas* transcriptomes from the top of colony biofilms, the bottom of colony biofilms,²³ whole drip flow biofilms,¹⁷ and planktonic cultures.²⁴

The microarray data discussed in this publication have been deposited in NCBI's Gene Expression Omnibus and are accessible through GEO Series accession number GSE75361 (<http://www.ncbi.nlm.nih.gov/geo/query/acc.cgi?acc=GSE75361>).

RESULTS

Biofilms formed by clinical isolates show steep oxygen gradients

Bacterial isolates from human chronic wounds formed biofilms when cultured in vitro. In the colony biofilm model using blood agar, isolates of *S. aureus*, *P. aeruginosa*, *E. faecalis*, and a combination of the three isolates, formed biofilms ranging from approximately 100 to 400 μm thick (Table 1). When profiled for oxygen concentration using microsensor technology, all of the biofilms exhibited steep gradients in oxygen concentration that diminished monotonically with increasing distance from the air interface of the biofilm (Figure 1). Note that in Figure 1, zero on the depth scale is arbitrary; microsensor measurements began in air above the biofilm and then the microsensor was lowered into the biofilm. The oxygen concentration began to decrease as the microsensor penetrated the biofilm. Though there were modest differences in the shapes of the concentration profiles, the results shown in Figure 1 are striking not for their differences but rather for their consistency. The membranes which supported the biofilms were oxygen permeable and presumably the growth medium contained oxygen. Nonetheless, bacteria from all three genera functioned similarly as oxygen sinks in this system, and depleted oxygen to less than 6.3 mmHg ($\sim 5\%$ of the oxygen concentration at the air-biofilm interface) within approximately 100 micrometers into the biofilm. Similar oxygen concentration profiles were measured in colony biofilms grown on dilute (10%) tryptic soy agar plates (data not shown).

Table 1. Colony biofilm characteristics and oxygen penetration depths

Species	Cell Density (log cfu/ membrane)	Thickness (μm)	O ₂ depth* (μm)
<i>P. aeruginosa</i>	9.08	130 \pm 13	71.7 \pm 7.3
<i>S. aureus</i>	8.68	162 \pm 14	108.7 \pm 3.9
<i>E. faecalis</i>	8.60	396 \pm 17	91.5 \pm 7.53
All three	9.10/7.17/8.05 [†]	281 \pm 13	110.4 \pm 5.0

*Oxygen penetration depth was calculated as the depth into the biofilm at which the pO₂ was <5% of the air above the biofilm.

[†]Cell density of *P. aeruginosa*, *S. aureus*, and *E. faecalis*, respectively, in the mixed-species biofilm.

Oxygen profiles from the scabs of mouse wounds infected with *P. aeruginosa* biofilms also show steep gradients

For in vivo wound oxygen measurements, a mouse model of delayed wound healing in which a full thickness punch wound on the back of the animal is inoculated with a preformed *P. aeruginosa* biofilm was utilized.^{13,14} Whereas noninfected wounds completely reepithelialized within 4 weeks, the biofilm-infected wounds typically required 6–8 weeks to close.^{13,14} As previously described, in this model, the bacteria are concentrated in the scab overlying the wound. These bacteria are in biofilms, as they are found in dense aggregates when examined microscopically and are tolerant to topical antibiotics. The transcriptome data described below also indicates that the cells are in biofilms. Thus, this model was used to determine oxygen concentrations in the vicinity of the biofilm (i.e., in the scab).

Wound scabs on immobilized, living mice harbored oxygen concentration gradients. Figure 2A shows typical profiles from wounds of two live mice. Note that in Figures 2 and 3, zero on the depth scales is arbitrary, microsensor measurements began in air above the scab or wound and then the microsensor was lowered into the scab or wound. The oxygen concentration began to decrease as the microsensor penetrated the scab or wound. The minimum oxygen concentration measured inside the scab in four independent measurements in two live mice, ranged from 17 to 72 mmHg with a mean value of 45. This was a mean decrease of 71% relative to the air above the scab. Similar measurements were made on intact wound scabs on euthanized animals (Figure 2B). In measurements from two different mice, the minimum oxygen concentrations were 6.4 and 1.1 mmHg. These values were lower than was observed in the living animals. Some of the oxygen concentration profiles measured in scabs in vivo exhibited minima (Figure 2). That is, with increasing distance into the scab, the oxygen concentration eventually increased, although often not back to initial values outside the scab. This feature was also observed in excised wound scabs from mice and human chronic wound specimens, but never observed in the in vitro grown biofilms (Figure 1). When

scabs were surgically removed and the underlying wound beds were probed, they were found to be relatively well oxygenated (Figure 2C). These profiles were similar to those measured in fresh wounds on live mice, which also showed very little oxygen depletion (Figure 2D).

A murine wound scab surgically removed from the animals and placed on agar plates was probed for oxygen concentration, and once again a steep oxygen concentration gradient was observed (Figure 3). The minimum oxygen concentration measured in the fresh ex vivo scab was 45 mmHg. When the scab was heated by microwaving, to inactivate bacteria and mouse cells, and subsequently probed again, oxygen concentration profiles were nearly flat. No obvious changes in the appearance of the scab were observed during or after microwaving. After microwaving, the minimum oxygen concentration ranged from 108 to 170 mmHg with a mean value of 142 mmHg. Concentration profiles measured in fresh ex vivo scabs sometimes exhibited a minimum in oxygen concentration, similar to profiles of the live mice.

Microelectrode profiles from ex vivo human chronic wounds also show oxygen gradients

Similar oxygen concentration profiles were observed within in vivo measurements on live mice and ex vivo measurements of excised scabs, indicating that the latter method might be suitable for investigating oxygen profiles in specimens from human chronic wounds. Debridement specimens were collected with a curette from two subjects at the Bozeman Health Wound and Lymphoma Center.

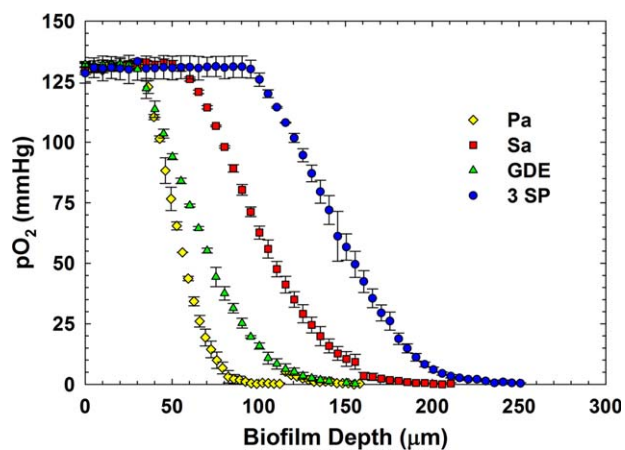


Figure 1. Oxygen concentration profiles in bacterial biofilms formed in vitro by human chronic wound isolates. Zero on the depth scale is arbitrary, microsensor measurements began in air above the biofilm and then the microsensor was lowered into the biofilm. The oxygen concentration began to decrease as the microsensor penetrated the biofilm. Each profile is the mean of three to four separate series of measurements, the error bars indicate standard deviations from the mean. Pa, *P. aeruginosa*; Sa, *S. aureus*; GDE, *E. faecalis*; 3 SP, mixed species biofilm of *P. aeruginosa*, *S. aureus*, and *E. faecalis*. Similar oxygen profiles were measured, regardless of the biofilm species composition. [Color figure can be viewed in the online issue, which is available at wileyonlinelibrary.com.]

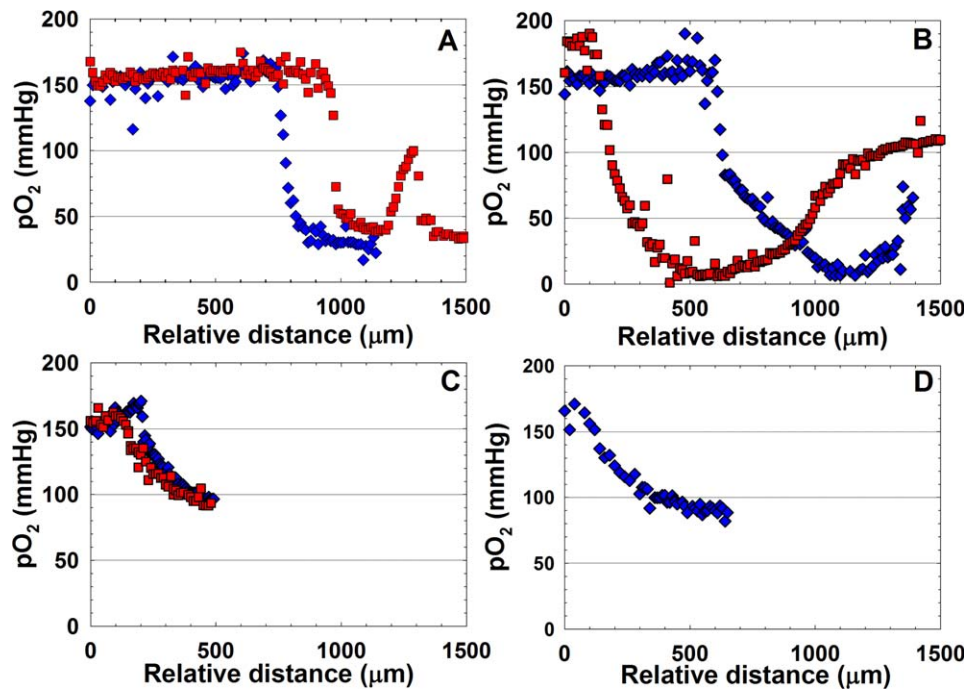


Figure 2. Oxygen concentration profiles in intact wound scabs on mice. The wounds were infected with *P. aeruginosa* biofilms two days post wounding. Zero on the depth scale is arbitrary, microsensors began in air above the scab or wound and then the microsensor was lowered into the scab or wound. The oxygen concentration began to decrease as the microsensor penetrated the scab or wound. (A) profiles from wound scabs of two different live mice. (B) Profiles from wound scabs of two different euthanized mice. (C) Profile from wound bed of living mouse after removal of the scab. (D) Profile from a fresh wound created on the back of a live mouse. Wound scabs had oxygen gradients similar to those observed in biofilms in vitro. [Color figure can be viewed in the online issue, which is available at wileyonlinelibrary.com.]

One subject had type 2 diabetes mellitus and was being treated for a foot ulcer. The other subject had idiopathic neuropathy and a nonhealing wound on a hammer toe. In both cases, the human debridement samples showed gradients of oxygen that decreased to as low as 1.60 mmHg (Figure 4). Note that in Figure 4, zero on the depth scale is arbitrary; microsensor measurements began in air above the specimen and then the microsensor was lowered into the specimen. Sequencing of PCR amplified 16S genes of subsamples of these specimens indicated the microbiota was predominated by *S. epidermidis* and other coagulase negative staphylococci and that *S. aureus* was also present.

Gene expression analysis of *P. aeruginosa* biofilms infecting mouse wounds shows that the bacteria are transcriptionally active and under hypoxia stress

Although human clinical isolates were used for the in vitro experiments described above, a well-characterized strain, *P. aeruginosa* mPAO1, with previously published planktonic and biofilm transcriptome data was used for the in vivo mouse infection model. In previous studies using this murine biofilm model, viable *P. aeruginosa* could be isolated from the wound scab 28 days postinfection, but at relatively low levels ($\sim 10^7$ cells/wound).^{13,14} In this study, we first confirmed the presence of *P. aeruginosa* in the wounds by isolating RNA from wound scabs and analyzing the presence of *P. aeruginosa* rRNA. Total RNA

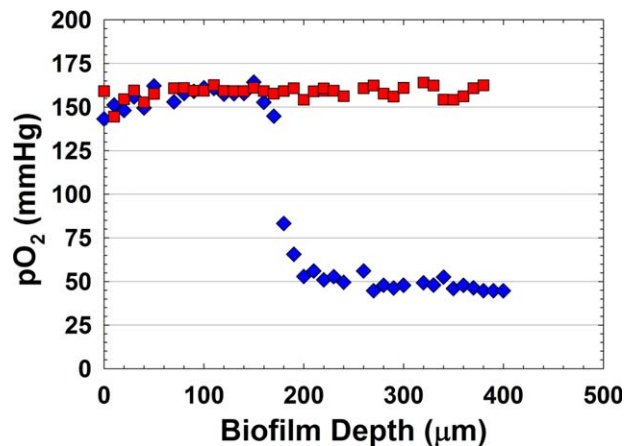


Figure 3. Oxygen concentration profiles in a murine wound scab probed ex vivo before (◆) or after (■) microwave heating. Zero on the depth scale is arbitrary, microsensor measurements began in air above the scab and then the microsensor was lowered into the scab. The oxygen concentration began to decrease as the microsensor penetrated the unheated scab. The wound scab retained an oxygen gradient after removal from the mouse. The oxygen gradient was eliminated by heating the scab, indicating that live bacteria were necessary for maintaining the gradient. [Color figure can be viewed in the online issue, which is available at wileyonlinelibrary.com.]

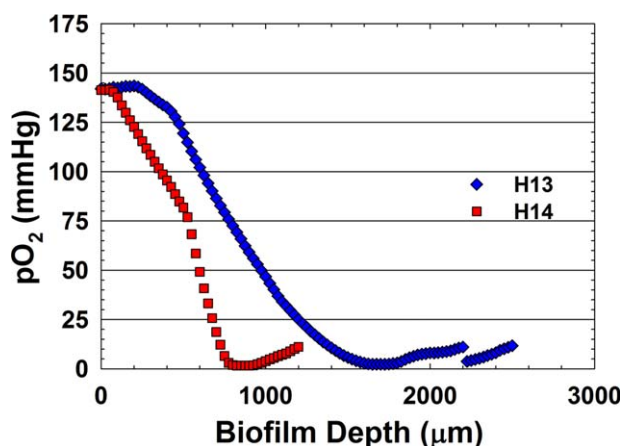


Figure 4. Oxygen concentration profiles in human wound debridement specimens. Zero on the depth scale is arbitrary, microsensor measurements began in air above the specimen and then the microsensor was lowered into the specimen. The oxygen concentration began to decrease as the microsensor penetrated the specimen. Each profile is the mean of three to four separate series of measurements, the error bars indicate standard deviations from the mean. Sample H13 was from a diabetic foot ulcer and Sample H14 was from a neuropathic toe ulcer. Human wounds had oxygen gradients similar to those observed for in vitro biofilms and experimental mouse wounds. [Color figure can be viewed in the online issue, which is available at wileyonlinelibrary.com.]

analysis of the wound scab using the Aligent Bioanalyzer showed four peaks associated with the rRNAs, including the 16S and 23S bacterial rRNAs and the 18S and 28S murine rRNAs. The Bioanalyzer results were verified by RT-qPCR using absolute quantification of the *P. aeruginosa* 16S rRNA. The RT-qPCR results indicated that intact *P. aeruginosa* RNA comprised approximately 20–24% of the total RNA (data not shown). These molecular analyses confirmed the bacterial culturing results, demonstrating that *P. aeruginosa* was present in the wounds 28 days postinfection. However, the molecular results do not distinguish between actively metabolizing cells and dormant bacteria. Ribosomal RNA within intact ribosomes has a long half-life compared with mRNA,²⁵ and therefore may be present in inactive bacteria. In addition, the culturing results performed previously do not distinguish between active and dormant bacteria. Therefore, we chose to assay the mRNA of the infecting bacteria using a microarray approach. mRNA has a short half-life, and therefore the presence of bacterial mRNA in the samples would suggest that the bacteria are transcriptionally active.

Although the number of bacterial cells within the wound scab was low for a microarray study, we chose to perform these transcriptome studies without the use of RNA amplification. This allowed us to identify those bacterial genes which were expressed abundantly in vivo, and to avoid the potential for amplification artifacts of mRNAs that are not present or found only at very low levels in the wound samples. As expected from the low amount of input RNA, most *P. aeruginosa* mRNA transcripts were below the detection limits by microarray analysis. However, internal

spike-in controls, hybridization controls, normal distribution of the data (Supporting Information Figure S1), and the positive correlation between the two arrays ($r^2 = 0.87$ for the linear regression), indicate that overall array quality was acceptable for analysis. We used a conservative analysis to identify the genes that had the most abundant expression in vivo. We first filtered out all genes that did not have a 2^6 or greater signal intensity in both biological samples. Of the remaining genes, the average signal intensity from both arrays was calculated to identify the most abundant 5% of transcripts from the total genes on the array. This resulted in a list of the 285 genes that had the most abundant expression in the mouse wound samples (Supporting Information Table S1).

A PCA was used to provide an overview of the transcriptome data from the 28-day mouse wound scab, comparing the data to the biofilm inoculum, and to published reports of *P. aeruginosa* biofilm and planktonic samples (Figure 5). The analysis shows that the transcriptome of the mouse wound scab was distinct from the biofilm inoculum that was applied to the wound, demonstrating a shift in biofilm gene expression following 28 days of infection. The transcriptome of the mouse wound also differed greatly from the transcriptomes of planktonic cells. Interestingly, the mouse wound biofilm transcriptome was most similar to the transcriptome of mature *P. aeruginosa* biofilms cultured in a drip flow reactor. In addition, comparing colony biofilms

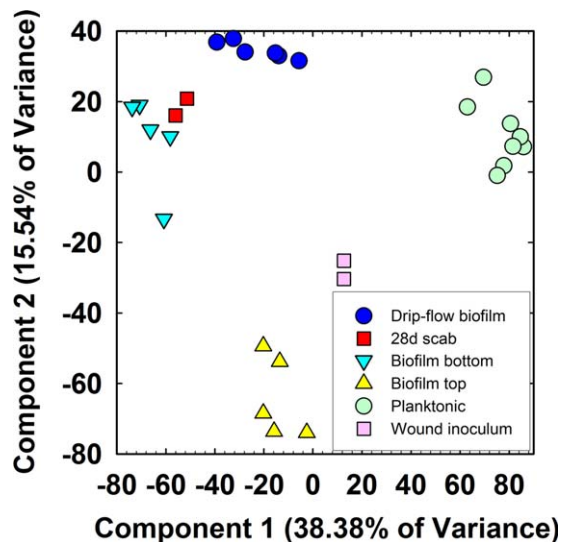


Figure 5. Principle component analysis of microarray data sets. PCA was used to visualize grouping of the mouse wound scab microarray data (dark square, this study) in comparison to published reference data sets. The reference data sets, all using *P. aeruginosa* strain PAO1, include a planktonic study (light circle),²⁴ a whole biofilm grown in a continuous flow biofilm reactor (dark circle),¹⁷ and specimens obtained from the active top (triangle up), and less active bottom (triangle down) of a colony biofilm.²³ Also included here is the colony biofilm preparation used as an inoculum in the mouse wound model (light square, this study). [Color figure can be viewed in the online issue, which is available at wileyonlinelibrary.com.]

Table 2. *P. aeruginosa* KEGG Pathways of genes most abundantly expressed in mouse wounds*

KEGG pathway [†]	Gene count	<i>p</i> -Value [‡]
Ribosome	28	1.8×10^{-30}
Pentose phosphate pathway	4	1.8×10^{-2}
Starch and sucrose metabolism	4	6.1×10^{-3}
RNA degradation	3	5.6×10^{-2}
Glycolysis/gluconeogenesis	4	5.6×10^{-2}
Purine metabolism	5	9.4×10^{-2}
Oxidative phosphorylation	5	5.0×10^{-2}

*Number of genes that fit in the KEGG pathways, from the 285 highest expressed genes in vivo.

[†]Pathway derived by DAVID analysis.

[‡]Probability that the cluster of genes associated with the pathway was derived by random chance.

where the transcriptome of the top and the bottom of the biofilms were analyzed separately, the PCA analysis indicated that these mouse scab biofilms grouped most closely with the bottom of colony biofilms, where cells have relatively low metabolic activity.²³

The list of 285 *P. aeruginosa* genes that were most abundantly expressed in vivo were also analyzed by DAVID to identify KEGG pathways for genes that were enriched in these samples (Table 2). Classes of transcripts that were enriched ($p < 0.1$) included genes involved in central metabolic energy-producing pathways: glycolysis, the pentose phosphate path-

way, and oxidative phosphorylation. Also enriched were genes for biosynthesis of ribosomes and for nucleic acid metabolism. Expression of these genes suggests that the bacteria from these wound samples, 28 days postinfection, were still metabolically active, and likely growing and engaging in oxygen-mediated or anaerobic respiration, as well as general housekeeping functions, such as ribosome and nucleic acid biosynthesis.

Examination of the list of the 285 highest-expressed *P. aeruginosa* genes in vivo indicated that the bacteria in these wound samples were engaged in various stress responses. In a separate study, we compiled lists of genes that are associated with particular stress responses, regulons, or common cellular functions, from literature reports.²² Here, we analyzed the list of 285 genes highly expressed in vivo in mouse wounds, for statistically significant overlap (at $p < 0.05$) with genes categorized with common functions or stress responses (Table 3 and Supporting Information Table S2). Strikingly, many genes enriched in these in vivo samples overlapped with genes associated with the Anr-mediated oxygen-limitation stress response (e.g., *arcABC*). The results are consistent with the low oxygen levels measured using the microsensors and suggest that the bacteria within these wounds also experience hypoxia. Genes regulated by the stationary phase sigma factor, RpoS, were also significantly enriched in the mouse scab biofilms, indicating that the bacteria may have been in a slow-growth or growth arrest state. Other groups of genes that were significantly enriched in expression were those associated with other stress responses, including osmotic shock and the RpoH-mediated heat shock response.

The consensus lists also indicated that the bacteria within these wounds were in a biofilm mode of growth, as genes for biofilm growth were significantly enriched in the

Table 3. Overlap of *P. aeruginosa* genes abundantly expressed in mouse wound samples with regulons or groups of related genes*

Regulon or functional group	Gene count [†]	Total on list [‡]	<i>p</i> -Value [§]	Reference
Osmotic shock	13	56	3.4×10^{-6}	31
Oxygen limitation	16	159	7.2×10^{-3}	24
Oxygen downshift	22	117	7.9×10^{-8}	32
Stationary phase	56	250	$<1.0 \times 10^{-14}$	24,32
Biofilm consensus	14	83	6.9×10^{-5}	17
MvfR regulon	31	115	4.3×10^{-15}	34
RpoH regulon	13	143	3.1×10^{-2}	Franklin, unpublished data
HSL quorum sensing	2	72	0.89	35,36
Cyclic-di-GMP	0	38	1.00	37
Iron limitation	4	61	0.38	38
Peroxide stress	4	48	0.23	39
Efflux pump	0	39	1.00	Pseudomonas.com
Virulence factors	13	195	0.20	Pseudomonas.com

*Number of genes from the 285 highest expressed genes in vivo that overlap with published regulons or related groups of genes.

[†]Number of highly expressed genes that overlap with a regulon or functional group.

[‡]Number of genes compiled from literature report of the regulon.

[§]Probability that the cluster of genes associated with the regulon was derived by random chance.

top 285 expressed genes (Table 3), further confirming the PCA results, which suggest that the scab biofilm transcriptomes are closely related to drip-flow biofilms. Other gene groups commonly associated with biofilm growth were not enriched in the mouse scab samples, including genes regulated by homoserine lactone-mediated quorum sensing and genes for cyclic-di-GMP metabolism. Other genes absent from enrichment included genes for iron limitation, efflux pumps, and virulence factors.

DISCUSSION

Very similar oxygen concentration profiles were found within single and mixed species biofilms grown *in vitro* as well as in scabs from experimental slow-healing biofilm-infected mouse wounds and in human chronic wounds. These results, as discussed in more detail below, support the hypothesis that biofilms contribute to the establishment and maintenance of localized low oxygen tensions in wounds. In the mouse wound scabs and human wound specimens, host cells such as neutrophils, responding to the presence of biofilm, probably also contributed to oxygen depletion. The generation of oxygen gradients and hypoxic conditions have negative impacts on wound healing.

Biofilms formed *in vitro* by bacteria isolated from human chronic wounds contained oxygen concentration gradients. Oxygen concentrations inside all of these biofilms dropped to less than 5% of the oxygen concentration at the air–biofilm interface over a distance of about one hundred microns. The concentration profiles measured in this work resemble those reported in many other microbial biofilm systems representing diverse environmental and medical contexts.^{17,26} The characteristic shape of these curves is determined by the interaction of reaction and diffusion.²⁷ The dense aggregation of bacteria in a biofilm creates both high volumetric respiration rates and restricted diffusion. These features in combination inevitably lead to oxygen concentration gradients.

The oxygen profiles shown in Figure 1 were measured within biofilms growing on a rich medium, blood agar. We measured similar profiles in colony biofilms grown on 10%-strength tryptic soy agar, a much lower nutrient medium. This comparison shows that the oxygen profiles are not very sensitive to the medium composition, just as they are not very sensitive to the species composition of the biofilm. We conclude that the ability of a biofilm to establish a steep oxygen concentration gradient is a robust characteristic of biofilm formation that extends to bacteria commonly encountered in human chronic wounds.

Measurements of oxygen concentration gradients within bacteria- and neutrophil-laden wound scabs from the mouse model were consistent with the presence of an oxygen sink within the scab (Figure 2A and B). This was likely by both consumption of oxygen by bacteria and due to the oxidative burst of neutrophils within the scab. Zhao et al. reported the presence of infiltrating neutrophils within scabs from this model.¹³ It has been previously suggested that excessive neutrophil accumulation in *P. aeruginosa*-infected wounds contributes to impaired wound healing.¹⁶ Indeed, Jesaitis et al. found that oxygen consumption *in vivo* was two- to fivefold higher in *P. aeruginosa* biofilm-neutrophil combinations than in the biofilms alone.²⁸ Oxygen profiles in scabs still adherent to mice (Figure 2A and B) and *in ex*

vivo scabs (Figure 3) were similar, indicating that oxygen consumption within the scabs was independent of direct interaction with the animal. The fact that heating the removed scab eliminated most of its ability to consume oxygen shows that oxygen consumption in the scab was an active metabolic process. Finally, measurements of oxygen concentrations in the wound bed after removal of the scab are not consistent with an oxygen sink within the animal tissue (Figure 2C). Oxygen supply to the wound bed is primarily through blood perfusion. This is evidenced by the observation that topical oxygen treatment resulted in a modest increase in pO₂ in superficial wound tissue, while systemic hyperbaric oxygen treatment resulted in large increases of tissue pO₂.⁷ The increase in oxygen concentration observed in profiles from the live and euthanized mice was in indication of oxygen being supplied to the wound bed. Similar increases were observed for excised scabs and human wound specimens, which may have been due to oxygen being supplied from the underlying agar. The presence of a scab containing most of the wound-associated bacteria, as well as neutrophils, in the mouse model is different than human chronic wounds where scabs are not often present. Nonetheless, the presence of oxygen gradients in human wound specimens suggest that similar oxygen sinks may be present at the surface of human chronic wounds.

The impact of a hypoxic biofilm on healing of well-oxygenated wounds is not clear from this study. The microsensor measurements indicated that the mouse wound beds of the *P. aeruginosa*-infected wounds were well oxygenated. Nonetheless, healing was delayed in these wounds relative to uninfected control wounds.^{13,14} The impact of a hypoxic biofilm may be even greater for wounds that have impaired blood perfusion due to vascular damage or ischemia. Certainly, the presence of strict anaerobes in chronic wounds^{7,8} indicate that hypoxic niches exist.

Pseudomonas aeruginosa biofilm and host interaction has been studied most extensively in relation to chronic lung infection in cystic fibrosis (CF) patients. Kolpen et al. reported that sputum samples from CF patients had low oxygen concentrations and a predominance of neutrophils, compared with other host cells, which was correlated with the number of *P. aeruginosa* present.¹⁵ The low sputum oxygen concentrations were attributed to the neutrophil respiratory burst. A study by Kragh et al. indicated that depletion of oxygen by neutrophils reduced the growth rate of *P. aeruginosa* in *ex vivo* CF lung specimens and *in vitro* experiments and that this stress could be alleviated by anaerobic respiration (denitrification) by the bacteria.²⁹ In human chronic wounds, neutrophils were also associated with *P. aeruginosa* biofilms, while wounds infected with *S. aureus* had fewer neutrophils. Wounds can be colonized or infected by a wide range of bacteria including complex polymicrobial biofilms. Consumption of oxygen by these biofilms, along with oxygen consumption by the host inflammatory response is likely a factor in the failure of chronic wounds to heal.

Transcriptional analysis of the wound scabs revealed that the bacteria within these wounds were actively growing and respiring. Genes expressed by these bacteria included transcripts for oxidative phosphorylation, ATP synthesis, TCA cycle enzymes, and glycolysis. Also abundant in the transcriptomes were genes for ribosome biosynthesis, suggesting that the cells were actively engaged in biosynthetic metabolic functions. While the transcriptome results suggest that *P. aeruginosa* cells were

metabolically active and likely consuming any available oxygen, the transcriptomes also indicated that the bacteria were under various stresses, and likely in a slow-growth stationary phase-like growth state. The PCA analysis indicated that the bacteria within the mouse wound scabs had a distinct expression profile from that of the biofilm inoculum and from previously characterized planktonic cells. In a separate study, we compared the transcriptomes of subpopulations of cells from within colony biofilms.²³ Interestingly, the PCA grouping of the mouse scab transcriptomes was closest to the transcriptomes of the bottom of *P. aeruginosa* colony biofilms. In our prior work, we used differential labeling and antibiotic tolerance studies to characterize the physiology of *P. aeruginosa* biofilm subpopulations.²³ Those results demonstrated that the cells at the bottom of colony biofilms were in a slow-growth and antibiotic tolerant state. The transcriptome results here may be used to infer that the biofilms of the mouse wounds are also in a slow-growth stationary-phase like growth state. These results are confirmed by the enrichment of genes from the RpoS-mediated stationary phase regulon, from the mouse scabs.

Anr is a regulatory protein that induces expression of genes during hypoxia stress.³⁰ Many of the genes that were highly expressed *in vivo* are under control of Anr-regulation. Therefore, the bacterial gene expression pattern serves as a biomarker for a low-oxygen state within the scabs, and is consistent with the microelectrode results. Among the genes under control of Anr are the arginine deiminase pathway (*arcABC*) genes, which are required for the utilization of arginine under low oxygen conditions. Other stress responses were also present in the transcriptomes of these samples, including osmotic stress (*osmC*), and heat shock stress (the *rpoH* sigma factor regulon). The RpoH regulon is induced by protein misfolding, and results in the induction of protein chaperones and proteases that refold or degrade misfolded proteins. The transcriptome results presented here, suggest that the bacteria must respond to protein misfolding, which is likely caused by the host defensive responses to the bacteria.

Genes for the biofilm mode of growth were significantly enriched in the transcriptomes of the mouse wounds (Table 3). Among the most abundantly expressed genes from this study were genes that had greater expression in biofilms than in planktonic cultures, suggesting that the bacteria within these wounds had physiological characteristics of biofilm bacteria. However, there was no evidence from the selected highly expressed transcripts in the wound of efflux pump production, elaboration of genes associated with cyclic-di-GMP metabolism, acyl homoserine lactone quorum sensing activity, or iron limitation. These results may have been due to the fact that most genes were expressed at very low levels, and therefore not detected using the microarray approach.

The results here support the hypothesis that bacterial biofilms in chronic wounds promote chronicity by contributing to the maintenance of localized low oxygen tensions. More specifically, we propose the following sequence of events involving chronic wounds: (1) The combination of injury and preexisting ischemia leads to hypoxic tissue niches. (2) These hypoxic niches are vulnerable to bacterial infection. Where oxygen levels are depressed, healing is slowed, and oxygen-dependent antibacterial pathways are impaired. (3) Once a biofilm has developed, it consumes available oxygen and attracts neutrophils. Invading neutrophils also consume oxygen and may even become the dominant oxygen sink.^{15,16} Through the combined oxy-

gen consumption of microorganisms and host cells, local oxygen concentrations are further diminished and anoxia is perpetuated. (4) The bacterial advantage is secured in the low oxygen/anoxic environment and healing is arrested. (5) The host inflammatory response, in concert with bacterial virulence factors, cause slow collateral damage to neighboring tissue and further impair healing. Since many different species of bacteria consume oxygen and could initiate this sequence, this model is consistent with the emerging consensus of the variable and polymicrobial nature of the microbial communities in chronic wounds.

ACKNOWLEDGMENTS

The authors thank James Marshall MHS, CWS, PA-C, Wound Clinic, Bozeman Health, for collecting the human wound debridement specimens. This research was supported in part by grant numbers 1P20GM078445-01, R21AI094268, RO1GM109452, and T32AR056969 from the National Institutes of Health (NIH) and the George F. Odland Endowed Research Fund. The contents of this report are solely the responsibility of the authors and do not necessarily represent the official views of the NIH.

REFERENCES

- Hunt TK, Zederfeldt B, Goldstick TK. Oxygen and healing. *Am J Surg* 1969; 118: 521–5.
- Sen CK. Wound healing essentials: Let there be oxygen. *Wound Repair Regen* 2009; 17: 1–18.
- Kalani M, Ostergren J, Brismar K, Jorneskog G, Fagrell B. Transcutaneous oxygen tension and toe blood pressure as predictors for outcome of diabetic foot ulcers. *Diabetes Care* 1999; 22: 147–51.
- Ruangsetakit C, Chinsakchai K, Mahawongkajit P, Wongwanit C, Mutirangura P. Transcutaneous oxygen tension: a useful predictor of ulcer healing in critical limb ischaemia. *J Wound Care* 2010; 19: 202–6.
- Gottrup F. Oxygen in Wound Healing and Infection. *World J Surg* 2004; 28, 312–5.
- Hopf HW, Hunt TK, West JM, Blomquist P, Goodson WH, Jensen JA, Jonsson, K, et al. Wound tissue oxygen tension predicts the risk of wound infection in surgical patients. *Arch Surg* 1997; 132: 997–1004.
- Trengove NJ, Stacey MC, McGechie, DF, Stingemore NF, Mata S. Qualitative bacteriology and leg ulcer healing. *J Wound Care* 1996; 5: 277–80.
- Dowd SE, Sun Y, Secor PR, Rhoads DD, Wolcott BM, James GA, et al. Survey of bacterial diversity in chronic wounds using pyrosequencing, DGGE, and full ribosome shotgun sequencing. *BMC Microbiol* 2008; 8: 43.
- Bjamsholt T, Kirketerp-Møller K, Jensen PØ, Madsen KG, Phipps R, Kroghfelt K, et al. Why chronic wounds will not heal: a novel hypothesis. *Wound Repair Regen* 2008; 16: 2–10.
- Watters C, DeLeon K, Trivedi U, Griswold JA, Lyte M, Hampel KJ, et al. *Pseudomonas aeruginosa* biofilms perturb wound resolution and antibiotic tolerance in diabetic mice. *Med Microbiol Immunol* 2013; 202: 131–41.
- Seth AK, Geringer MR, Galiano RD, Leung KP, Mustoe TA, Hong SJ. Quantitative comparison and analysis of species-specific wound biofilm virulence using an *in vivo*, rabbit-ear model. *J Am Coll Surg* 2012; 215: 388–99.

12. Trøstrup H, Thomsen K, Christophersen LJ, Hougen HP, Bjarnsholt T, Jensen PØ, et al. *Pseudomonas aeruginosa* biofilm aggravates skin inflammatory response in BALB/c mice in a novel chronic wound model. *Wound Repair Regen* 2013; 21: 292–9.
13. Zhao G, Hochwalt PC, Usui ML, Underwood RA, Singh PK, James GA, et al. Delayed healing in diabetic (db/db) mice with *Pseudomonas aeruginosa* biofilm challenge: a model for the study of chronic wounds. *Wound Repair Regen* 2010; 18: 467–77.
14. Zhao G, Usui ML, Underwood RA, Singh PK, James GA, Stewart PS, et al. Time course study of delayed wound healing in a biofilm-challenged diabetic mouse model. *Wound Repair Regen* 2012; 20: 342–52.
15. Kolpen M, Hansen CR, Bjarnsholt T, Moser C, Christensen LD, van Gennip M, et al. Polymorphonuclear leukocytes consume oxygen in sputum from chronic *Pseudomonas aeruginosa* pneumonia in cystic fibrosis. *Thorax* 2010; 65: 57–62.
16. Fazli M, Bjarnsholt T, Kirketerp-Møller K, Jørgensen A, Bgelund Andersen C, Givskov M, et al. Quantitative analysis of the cellular inflammatory response against biofilm bacteria in chronic wounds. *Wound Repair Regen* 2011 19: 387–391.
17. Folsom JP, Richards L, Pitts B, Roe F, Ehrlich GD, Parker A, et al. Physiology of *Pseudomonas aeruginosa* in biofilms as revealed by transcriptome analysis. *BMC Microbiol* 2010; 10: 294.
18. Lewandowski Z, Beyenal H. *Fundamentals of Biofilm Research*. Boca Raton: CRC Press, 2007.
19. Pérez-Osorio AC, Williamson KS, Franklin MJ. Heterogeneous rpoS and rhlR mRNA levels and 16S rRNA/rDNA ratios within *Pseudomonas aeruginosa* biofilms, sampled by laser capture microdissection. *J Bacteriol* 2010; 192: 2991–3000.
20. Blazejczyk M, Miron M, Nadon R. *FlexArray: A Statistical Data Analysis Software for Gene Expression Microarrays*. Montreal: Genome Quebec, 2007.
21. Huang DW, Sherman BT, Lempicki RA. Systematic and integrative analysis of large gene lists using DAVID Bioinformatics Resources. *Nature Protoc* 2009; 4: 44–57.
22. Stewart PS, Franklin MJ, Williamson KS, Folsom JP, Laura Boegli, James GA. Contributions of stress response to antibiotic tolerance in *Pseudomonas aeruginosa* biofilms. *Antimicrob Agents Chemother* 2015; 59: 3838–47.
23. Williamson KS, Richards LA, Perez-Osorio AC, Pitts B, McInerney K, Stewart PS, et al. Heterogeneity in *Pseudomonas aeruginosa* biofilms includes expression of ribosome hibernation factors in the antibiotic-tolerant subpopulation and hypoxia-induced stress response in the metabolically active population. *J Bacteriol* 2012; 194: 2062–73.
24. Alvarez-Ortega C, Harwood CS. Responses of *Pseudomonas aeruginosa* to low oxygen indicate that growth in the cystic fibrosis lung is by aerobic respiration. *Mol Microbiol* 2007; 65: 153–65.
25. Deutscher MP. Degradation of stable RNA in bacteria. *J Biol Chem* 2003; 278: 45041–4.
26. de Beer D, Stoodley P, Roe F, Lewandowski Z. Effects of biofilm structure on oxygen distribution and mass transport. *Biotechnol Bioeng* 1994; 43: 1131–8.
27. Stewart PS. Diffusion in biofilms. *J Bacteriol* 2003; 185: 1485–91.
28. Jesaitis AJ, Franklin MJ, Berglund D, Sasaki M, Lord CI, Bleazard JB, et al. Compromised host defense on *Pseudomonas aeruginosa* biofilms: characterization of neutrophil and biofilm interactions. *J Immunol* 2003; 171: 4329–39.
29. Kragh KN, Alhede M, Jensen PØ, Moser C, Scheike T, Jacobsen CS, et al. Polymorphonuclear leukocytes restrict growth of *Pseudomonas aeruginosa* in the lungs of cystic fibrosis patients. *Infect Immun* 2014; 82: 4477–86.
30. Trunk K, Benkert B, Quack N, Munch R, Scheer M, Garbe J, et al. Anaerobic adaptation in *Pseudomonas aeruginosa*: definition of the Anr and Dnr regulons. *Environ Microbiol* 2010; 12: 1719–23.
31. Aspedon A, Palmer K, Whiteley M. Microarray analysis of the osmotic stress response in *Pseudomonas aeruginosa*. *J Bacteriol* 2006; 188: 2721–5.
32. Lequette Y, Lee J-H, Ledgham F, Lazdunski A, Greenberg EP. A distinct QscR regulon in the *Pseudomonas aeruginosa* quorum-sensing circuit. *J Bacteriol* 2006; 188: 3365–70.
33. Teitzel GM, Geddie A, De Long SK, Kirisits MJ, Whiteley M, Parsek MR. Survival and growth in the presence of elevated copper: transcriptional profiling of copper-stressed *Pseudomonas aeruginosa*. *J Bacteriol* 2006; 188: 7242–56.
34. Déziel E, Gopalan S, Tampakaki AP, Lépine F, Padfield KE, Saucier M, et al. The contribution of MvfR to *Pseudomonas aeruginosa* pathogenesis and quorum sensing circuitry regulation: multiple quorum sensing-regulated genes are modulated without affecting lasRI, rhlRI or the production of N-acyl-L-homoserine lactones. *Mol Microbiol* 2005; 55: 998–1014.
35. Schuster M, Lostroh CP, Ogi T, Greenberg EP. Identification, timing, and signal specificity of *Pseudomonas aeruginosa* quorum-controlled genes: a transcriptome analysis. *J Bacteriol* 2003; 185: 2066–79.
36. Wagner VE, Bushnell D, Passador L, Brooks AI, Iglewski BH. Microarray analysis of *Pseudomonas aeruginosa* quorum-sensing regulons: effects of growth phase and environment. *J Bacteriol* 2003; 185: 2080–95.
37. Kulasekara BR, Kulasekara HD, Wolfgang MC, Stevens L, Frank DW, Lory S. Acquisition and evolution of the exoU locus in *Pseudomonas aeruginosa*. *J Bacteriol* 2006; 188: 4037–50.
38. Ochsner UA, Wilderman PJ, Vasil AI, Vasil ML. Gene-Chip expression analysis of the iron starvation response in *Pseudomonas aeruginosa*: identification of novel pyoverdine biosynthesis genes. *Mol Microbiol* 2002; 45: 1277–87.
39. Palma M, DeLuca D, Worgall S, Quadri L. Transcriptome analysis of the response of *Pseudomonas aeruginosa* to hydrogen peroxide. *J Bacteriol* 2004; 186: 248–52.

Supporting Information

Additional Supporting Information may be found in the online version of this article at the publisher's web-site:

Table S1. List of the 285 genes that had the most abundant expression in the mouse wound samples.

Table S2. Gene sets associated with stress responses or hypothesized protective mechanisms in *Pseudomonas aeruginosa* PAO1.

Figure S1. Histograms of microarray data from the two mouse wound samples.